Cite as: Li XJ, Zhao GJ, Ren JH. Application of dual-modality ultrasound deep learning predictive model in diagnosing breast cancer [J]. Chin J Clin Res, 2024, 37(3): 365-369, 374.
DOI: 10.13429/j. cnki.cjcr.2024.03.008

Application of dual-modality ultrasound deep learning predictive model in diagnosing breast cancer

LI Xiaojie*, ZHAO Guojia, REN Jinhe

*Graduate School of Jinzhou Medical University, Jinzhou Liaoning 121000, China

Corresponding author: REN Jinhe, E-mail: renjh8677@163.com

Abstract: Objective To develop a predictive model using deep learning (DL) techniques based on breast ultrasound grayscale images and ultrasound elastography, and to explore the diagnostic efficacy of this model in differentiating benign from malignant breast lesions. **Methods** A retrospective collection was made of data from 1 000 breast lesions that underwent surgical treatment at Linyi People's Hospital Breast Surgery Department from May 2020 to April 2021, including ultrasound images and related clinical pathological information. The ultrasound grayscale images and ultrasound elastography of the largest section of each lesion were selected and randomly divided into training, validation, and test sets at a ratio of 7:2:1. A predictive model was constructed based on neural networks using the training and validation sets, and the diagnostic efficacy of the model was tested with the test set images. Four ultrasound physicians were invited to read the test set ultrasound images independently, and their diagnostic efficacies were compared with the model's performance. **Results** The area under the curve (AUC) value (0.907) of the receiver operating curve (ROC) of DL model for breast lesion diagnosis was higher than all participating physicians, with a statistically significant difference (P<0.05). The average AUC value for the diagnosis by senior physicians (0.835) was higher than that for junior physicians (0.719), with a statistically significant difference (P<0.05). When the model assisted junior physicians and senior physicians in diagnosing the test set breast lesions, the average AUC value was 0.806 and 0.864, respectively. After assistance from the model, the diagnostic efficacy of physicians of different experience levels improved, with a more significant increase for junior physicians (P<0.05). Notably, there was no statistically significant difference in the AUC values between the junior physicians assisted by the DL model and the senior physicians reading alone (P>0.05). **Conclusion** A predictive model based on dual-modality ultrasound DL can significantly improve the diagnostic efficacy of physicians in differentiating benign from malignant breast lesions.

Keywords: Deep learning; Neural network; Breast cancer; Ultrasound; Elastic imaging; Prediction model; Artificial intelligence

Breast cancer is the most common cancer in females worldwide, with a relatively high mortality and an increasing incidence at younger ages. Early and accurate diagnosis is crucial [1-2]. Ultrasound plays an important role in the diagnosis and treatment of breast cancer [3]. Breast ultrasound has a high diagnostic value in revealing basic characteristics such as morphology, margins, growth patterns and internal echoes of breast lesions [4]. Strain elastography (SE) reflects hardness within breast lesions and surrounding normal tissues, improving the specificity and accuracy of breast cancer diagnosis and decreasing the rate of preoperative breast biopsy [5-7]. However, ultrasound examinations are subjective, especially in determining ultrasound characteristics and assessing hardness. The results vary according to the skills and experience of different physicians [8]. In recent years, computer-aided diagnosis (CAD) based on deep learning (DL) has developed rapidly and played an essential role in medical image processing and analysis, including breast, thyroid, lung and brain imaging [9-12]. This study aims to construct a predictive model of breast lesions using DL techniques based on greyscale images combined with ultrasound elastography, and to evaluate its potential to assist physicians in improving diagnostic accuracy.

1. Data and methods

1.1 General data

This retrospective study collected data from 888 patients with breast disease who underwent surgery at the Linyi People's Hospital Breast Surgery Department from May 2020 to May 2021. The age of the patients ranged from 13 to 81 (44.6±11.8) years. A total of 1,000 lesions with pathological diagnoses were included, including 600 benign and 400 malignant cases. Inclusion criteria required clear and complete ultrasound images showing breast lesions and comprehensive clinical and pathological data. This study retrospectively analyzed the established clinical imaging and pathological data of the patients, without interfering with the clinical diagnosis and treatment, and protecting the privacy of the patients. This study complied with ethical principles and was exempt from ethical review.

1.2 Ultrasound Images

A GE LogiqE9 ultrasound transducer with a ML6-15-D wideband matrix linear array probe (6-15 MHz) equipped with SE was used. Ultrasound elastic images of the largest section diameter for each breast lesion were selected and 1,000 images were randomly divided into training (*n*=700), validation (*n*=200) and test (*n*=100) sets in a ratio of 7:2:1, with a ratio of benign to malignant cases of 3:2 for each set.

1.3 Image pre-processing

Images were cropped based on the sampling frame size of the elastography, extracting ultrasound grayscale images and ultrasound elastography including the lesions and surrounding normal tissue structures. Irrelevant information such as hospitals and details of patients, imaging parameters and anatomic marks were removed for model input. **[Figure 1]**.

1.4 Building of the predictive model

ResNet-101 was used to extract different characteristic parameters from ultrasound grayscale images and ultrasound elastography. A multi-layer adaptive feature fusion module was added to the network structure to merge the feature maps of the ultrasound grayscale images and the ultrasound elastography. Finally, a fully connected layer was used for binary classification of benign and malignant lesions. **[Figure 2].** A total of 700 lesion grayscale images and elastography in the training set were simultaneously fed into the model for parameter training, with each image having accurate labels for benign and malignant lesions. The validation set of 200 lesion images was used to optimize and adjust the model parameters. A 5-point elastography scoring method obtained the DL model with the optimal diagnostic value. Model training was performed using Pytorch 1.2.0 on the NVIDIA GeForce RTX 2080 8GB GPU platform.

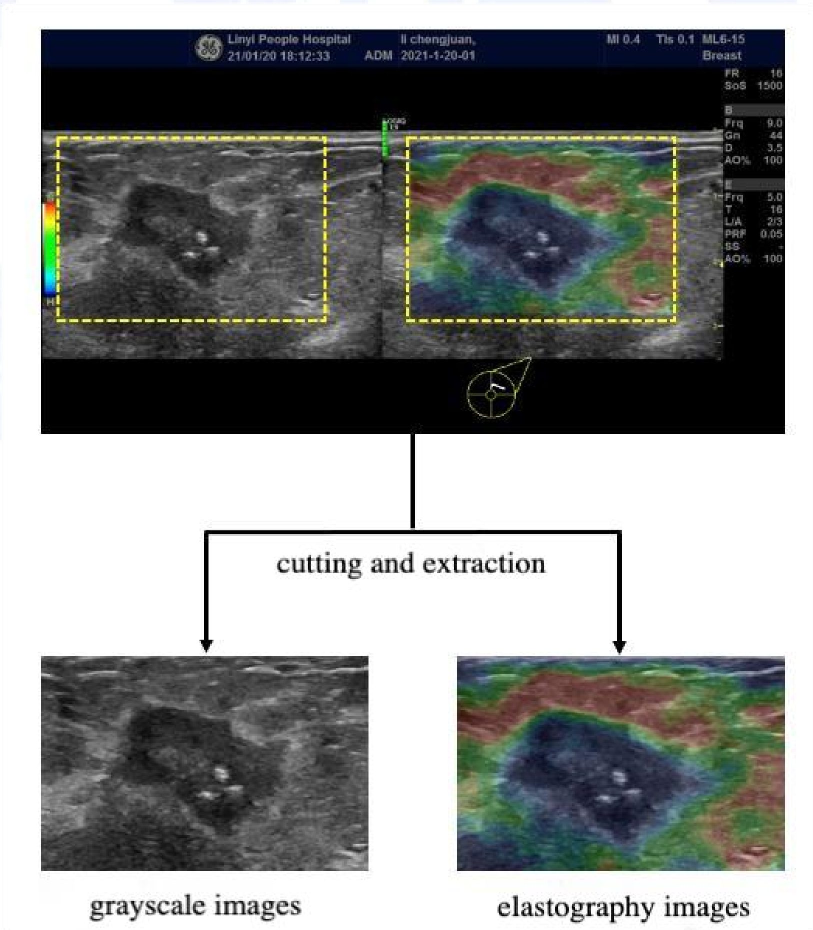

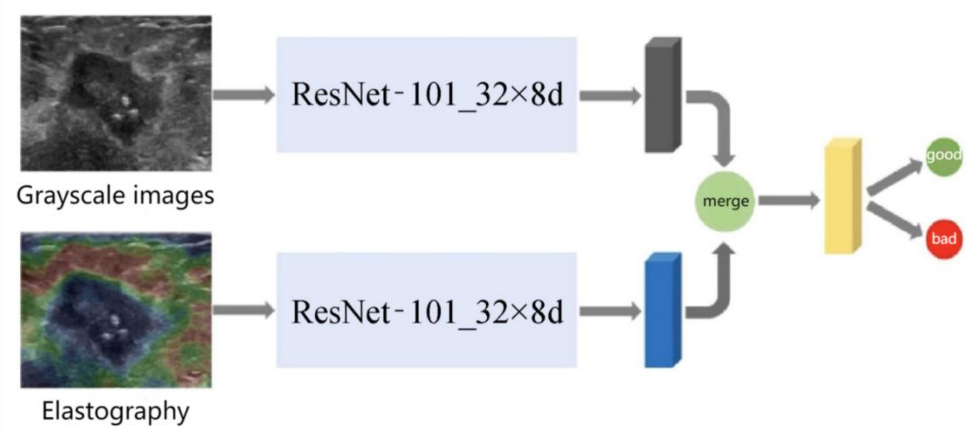

1.5 Model testing

Grayscale images and elastography of 100 breast lesions from the test set were randomly input into the DL model for diagnostic evaluation. The diagnostic performance of the model was assessed and the output consisted of prediction probability of malignancy for each lesion (ranging from 0 to 1). Using a threshold of 0.5, If the prediction probability exceeds 0.5, the sample is predicted to be malignant and labeled as 1; otherwise, benign and labeled as 0.

1.6 Review of physicians

Four ultrasound physicians with different experience levels participated in a double-blind review of the ultrasound images. Physicians 1 and 2, with 15 and 11 years of breast ultrasound diagnostic experience, were categorized as senior physicians. Physicians 3 and 4, with 3 and 2 years of experience, were categorized as junior physicians.

The review cases included ultrasound grayscale and elastography of 100 breast lesions from the test set. Four physicians reviewed each lesion's ultrasound images for diagnosis in each of the following two scenarios: (1) independent review without DL model assistance and (2) review with DL model assistance. The interval between the two reviews was 4 weeks. When assisted by the DL model, physicians could consider the model's prediction probability of malignancy and corresponding diagnosis, then accept or reject the model's diagnosis to make their final decision.

1.7 Statistical analysis

SPSS 26.0 and MedCalc 14.0 were used for data analysis. General characteristics of benign and malignant breast lesions were compared using the Mann-Whitney *U* test. Pathological diagnosis results from the test set were used as the gold standard. Sensitivity, specificity, accuracy, positive and negative predictive values were calculated for the DL model and the four ultrasound physicians. Receiver operating characteristic (ROC) curves were plotted and the area under the curve (AUC) was calculated. Differences in diagnostic performance between the model and the different physicians were compared using DeLong's test. A significance level of $P<0.05$ was considered statistically significant.

2. Results

2.1 General characteristics of patients with breast diseases and lesions

The characteristic distribution of breast lesions in the training and test sets was similar. Patients with benign lesions were significantly younger than those with malignant lesions ($P<0.01$). Malignant lesions were significantly larger in section diameter than benign lesions ($P<0.01$). The pathological type distribution of benign and malignant lesions is shown in **Table 1**.

2.2 Comparison of DL model and diagnostic efficacy of physicians with different seniority alone or in combination

The accuracy, sensitivity, specificity, positive predictive value, and negative predictive value of the DL model and physicians of different seniority in diagnosing 100 lesions from the test set based on grayscale images and elastography are shown in **Table 2**. ROC curves for the DL model and physicians' diagnostic results were plotted, and the area under the curve (AUC) values for each curve were calculated and compared. The results indicate: (1) the AUC value of the DL model for diagnosing breast lesions is higher than that of all physicians, with a statistically significant difference ($P<0.05$); (2) AUC values of independent reviews of senior physicians are higher than those of junior physicians, with statistical significance ($P<0.05$).

2.3 Comparison of efficacy in DL model-assisted and independent medical reviews

The accuracy, sensitivity, specificity, positive predictive value and negative predictive value of model-assisted and independent medical review are shown in **Table 2**. ROC curves were plotted for both scenarios, and AUC values were calculated and compared. The results indicate: (1) the diagnostic performance of physicians with different levels of experience improved after model-assisted reviews, especially for junior physicians, with a statistically significant difference (P<0.05); the improvement in AUC values for senior physicians was limited and not statistically significant (P>0.05); (2) model-assisted reviews of junior physicians achieved diagnostic performance comparable to independent reviews by senior physicians, with no statistically significant difference in AUC values (P>0.05). **[Figure 4]**.

Tab.1 General characteristics of breast disease patients and lesions [case(%)]

Items	Trainingsets+validationsets		Testsets	
	Benign	Malignant	Benign	Malignant
Number of lesions	540	360	60	40
Number of images [a]	1080	720	120	80
Largest section diameter	16±8	24±10	19±9	26±12
< 10 mm	90(16.7)	22(6.1)	3(5.0)	3(7.5)
10-40 mm	443(82.0)	305(84.7)	55(91.7)	30(750.0)
> 40 mm	7(1.3)	33(9.2)	2(3.3)	7(17.5)
BI-RADS classification				
3	386(71.5)	5(1.4)	41(68.3)	0
4a	118(21.9)	34(9.4)	14(23.3)	5(12.5)
4b	32(5.9)	81(22.5)	4(6.7)	9(22.5)
4c	4(0.7)	177(49.2)	1(1.7)	21(52.5)
5	0	63(17.5)	0	5(12.5)
Pathological diagnosis				
Fibroadenoma	405(75.0)		36(60.0)	
Adenopathy	79(14.6)		9(15.0)	
Intraductal papilloma	27(5.0)		3(5.0)	
Mastitis	14(2.6)		5(8.3)	
Sclerosing adenosis	5(0.9)		5(8.3)	
Fat necrosis	5(0.9)		1(1.7)	
Phyllodes tumour	2(0.4)		1(1.7)	
Invasive ductal carcinoma		291(80.3)		34(85.0)
Ductal carcinoma *in situ*		53(14.7)		3(7.5)
Mucinous carcinoma		6(1.7)		1(2.5)
Mixed invasive carcinoma		4(1.1)		1(2.5)
Invasive lobular carcinoma		2(0.6)		1(2.5)
Others	3(0.6)	4(1.1)	0	0

Note:[a] each lesion has both grayscale images and elastography.

Tab.2 Comparison of diagnostic performance of DL model and physicians with different years of experience, either alone or in combination (%)

Item	Sensitivity	Specificity	Accuracy	Positive predictive value	Negative predictive value	AUC
DL model	82.5	83.3	83.0	87.7	76.7	0.907
Physician 1	87.5	81.6	84.0	76.1	90.7	0.846
Physician 2	85.0	80.0	82.5	73.9	88.9	0.825
Physician3	73.3	70.0	72.0	63.6	78.5	0.721
Physician 4	57.5	81.6	72.0	67.6	74.2	0.717
DL+Physician 1	90.0	85.0	87.0	80.0	92.7	0.875
DL+Physician 2	87.5	83.3	85.0	77.7	90.9	0.854
DL+Physician 3	80.0	81.6	81.0	74.4	85.9	0.804
DL+Physician 4	82.5	78.3	80.0	71.7	87.0	0.808

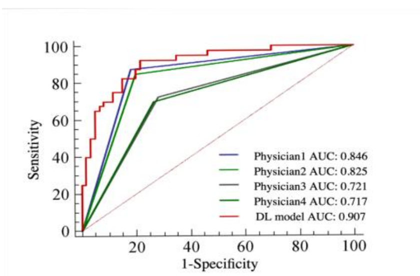

Fig.3 ROC curves of diagnostic performance of DL model and physicians with different years of experience

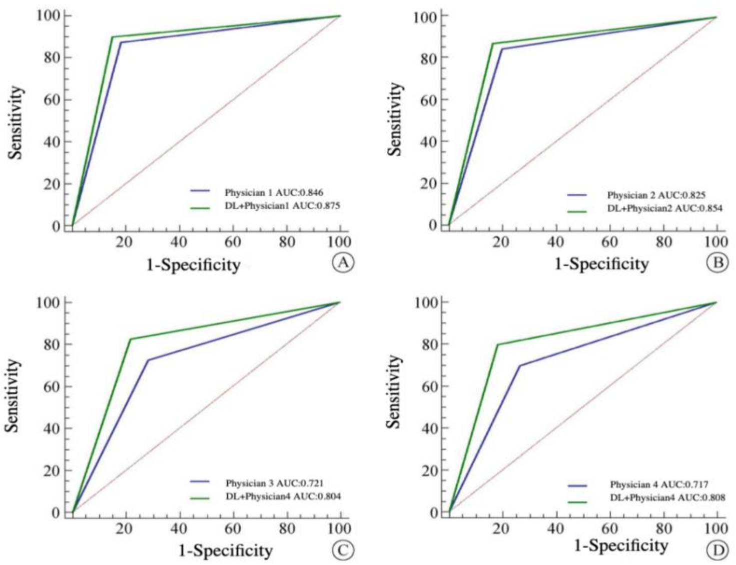

Fig.4 ROC curve of the diagnostic performance of DL model in assisting physicians in reading films and physicians reading films individually

3 Discussion

Breast ultrasound is widely used in clinical practice. Ultrasound elastography can improve the diagnostic accuracy of breast cancer by reflecting the hardness of lesions and surrounding normal tissues [4,13]. The DL model constructed in this study achieved satisfactory results in the classification of benign and malignant breast lesions.

The basic principle of convolutional neural networks (CNNs) is to train a kernel to recognize specific features (convolutional layer). The convolutional layer calculates the degree of overlap among features between the kernel and the input images (called the receptive field). Subsequently, pooling layers and fully connected layers flatten the data into eigenvectors. The output layer computes the probability of output classes using a dense network and a regression function [14]. CNN can analyze image features at a more detailed and pixel-level dimension, leading to more accurate diagnoses. In recent years, many scholars have developed single-DL models for breast lesion diagnosis, showing high consistency with expected results. It was found that using CAD based on conventional 2D ultrasound images to diagnose 266 breast lesions achieved an AUC of 0.81, which was not significantly different from that of senior ultrasound physicians (AUC=0.82), but higher than that of junior ultrasound physicians with an AUC of 0.76 [15]. Li *et al.* [16] built a DL model based on a large data set of breast lesions and found diagnostic performance equivalent to that of ultrasound experts and significantly superior to that of junior physicians (AUC=0.66-0.71, $P<0.05$). However, models based on 2D greyscale images of breast lesions alone provide limited information. In this study, elastography information was involved to improve diagnostic performance.

A Meta-analysis by Wu *et al.* [17] found that the use of strain elastography to diagnose breast lesions resulted in an AUC of 0.899. Golatta *et al.* [18] found that the addition of elastography to conventional ultrasound for the diagnosis of 4a lesions in 1,288 women with BI-RADS ultrasound subcategories of 3 to 4c had a positive impact on the diagnosis of breast lesions. The number of unnecessary biopsies in breast diagnosis was reduced by approximately 35.35%, while the leak detection rate of malignancy was maintained at 1.96%. All of the above indicates that the use of breast elastography can provide richer texture information on lesions, morphological features and information on hardness, which can enrich the diagnostic basis of the ultrasound physicians and thus achieve a more efficient and accurate diagnosis. In clinical practice, there are subjective and repeated differences in the diagnosis of solid breast lesions, whether by the elastography 5-point score or strain ratio method [19-20]. In order to improve diagnostic accuracy, timeliness and reduce intra-observer variability, CAD systems are gradually being introduced into breast ultrasound. In this study, the DL model based on 2D grayscale images and strain elastography of breast lesions showed satisfactory results in lesion classification, outperforming physicians with different levels of experience (AUC values for the DL model and physicians ranged from 0.907 to 0.717-0.846). Consistent with our findings, studies by Misra [21], Zhang [22] and others show that dual-DL models have a high diagnostic value for benign and malignant classification of breast lesions. Therefore, it is believed that dual-DL models incorporating elastography have superior capabilities for breast lesion classification compared to single DL models using only conventional 2D grayscale images.

In this study, DL models assisted physicians in diagnosing breast lesions by allowing them to choose between the model results and their initial diagnoses when disagreed. The results showed improved AUC values for physicians after DL model assistance (mean AUC values before and after assistance were 0.777 and 0.835, respectively, $P<0.05$). Choi *et al.* [23] asked four physicians to classify 253 breast lesions using BI-RADS, and when the DL models were added to conventional ultrasound, the AUC values (0.91-0.95) were significantly higher than the AUC values (0.88-0.92) using conventional ultrasound images alone. Wang *et al.*[24] added CAD and SE to conventional ultrasound, which resulted in a significant increase in the AUC value from 0.72 to 0.91. In conclusion, using the DL model to assist physicians in ultrasound diagnosis can improve the diagnostician's decision-making to some extent, reduce the number of missed and misdiagnosed diagnoses, and improve the detection rates of breast cancer.

Although the DL model in this study showed a high diagnostic value in distinguishing benign from malignant breast lesions, there are some limitations: (1) the model only included grayscale and elastography information, neglecting factors such as blood flow measurements, contrast-enhanced ultrasound and dynamic imaging. (2) breast lesions are 3D structures, but this study only included 2D grayscale and elastography images, not including coronal sections of tumors, which may introduce bias due to the subjective nature of the ultrasound physicians during image acquisition. (3) the study focused on images of space-occupying lesions, potentially leading to an overestimation of the diagnostic performance.

Combining conventional breast ultrasound with CAD and DL technology can address missed diagnoses and misdiagnoses due to insufficient physicians' experience and skills, ultimately improving diagnostic efficiency. Applying DL methods with robust learning capabilities and efficient classification to routine detection and classification of breast ultrasound lesions in hospitals holds great promise.

Conflict of interest None

References

[1] Sung H, Ferlay J, Siegel RL, et al. Global cancer statistics 2020: GLOBOCAN estimates of incidence and mortality worldwide for 36 cancers in 185 countries[J]. CA Cancer J Clin, 2021, 71(3): 209-249.

[2] He J, Chen WQ, Li N, et al. China guideline for the screening and early detection of female breast cancer(2021, Beijing)[J]. Chin J Oncol, 2021, 43(4): 357-382. **[In Chinese]**

[3] Berg WA, Bandos AI, Mendelson EB, et al. Ultrasound as the primary screening test for breast cancer: analysis from ACRIN 6666[J]. J Natl Cancer Inst, 2015, 108(4): djv367.

[4] Zanello PA, Robim AFC, Oliveira TM, et al. Breast ultrasound diagnostic performance and outcomes for mass lesions using Breast Imaging Reporting and Data System category 0 mammogram[J]. Clinics, 2011, 66(3): 443-448.

[5] Pfob A, Sidey-Gibbons C, Barr RG, et al. Intelligent multi-modal shear wave elastography to reduce unnecessary biopsies in breast cancer diagnosis (INSPiRED 002): a retrospective, international, multicentre analysis[J]. Eur J Cancer, 2022, 177: 1-14.

[6] Zhao QY, Zhao B, Wu G, et al. Value of quantitative parameters of ultrasound shear wave elastography to the prediction of loco-regional recurrence of breast cancer after systemic therapy[J]. J Chin Pract Diagn Ther, 2023, 37(4): 377-382. **[In Chinese]**

[7] Dong M, Zhang BY, Xing BY. Application progress of ultrasound elastography in breast diseases[J]. China Med Her, 2022, 19(22): 42-45, 61. **[In Chinese]**

[8] Secco GM, Gutierrez PA, Secco VL, et al. Is breast ultrasound a good alternative to magnetic resonance imaging for evaluating implant integrity?[J]. Radiologia, 2022, 64(Suppl 1): 20-27.

[9] Yoon J, Lee HS, Kim MJ, et al. AI-CAD for differentiating lesions presenting as calcifications only on mammography: outcome analysis incorporating the ACR BI-RADS descriptors for calcifications[J]. Eur Radiol, 2022, 32(10): 6565-6574.

[10] Xie F, Luo YK, Lan Y, et al. Differential diagnosis and feature visualization for thyroid nodules using computer-aided ultrasonic diagnosis system: initial clinical assessment[J]. BMC Med Imaging, 2022, 22(1): 153.

[11] Shafi I, Din S, Khan A, et al. An effective method for lung cancer diagnosis from CT scan using deep learning-based support vector network[J]. Cancers, 2022, 14(21): 5457.

[12] Ishihara M, Shiiba M, Maruno H, et al. Detection of intracranial aneurysms using deep learning-based CAD system: usefulness of the scores of CNN's final layer for distinguishing between aneurysm and infundibular dilatation[J]. Jpn J Radiol, 2023, 41(2): 131-141.

[13] Wang HX, Long ST, Song ZJ, et al. Ultrasound-guided localization technique in the diagnosis of breast tumors[J]. Chin J Clin Res, 2022, 35(9):1227-1232.**[In Chinese]**

[14] Mao YJ, Lim HJ, Ni M, et al. Breast tumour classification using ultrasound elastography with machine learning: a systematic scoping review[J]. Cancers, 2022, 14(2): 367.

[15] Litjens G, Kooi T, Bejnordi BE, et al. A survey on deep learning in medical image analysis[J]. Med Image Anal, 2017, 42: 60-88.

[16] Li JM, Bu YY, Lu SQ, et al. Development of a deep learning-based model for diagnosing breast nodules with ultrasound[J]. J Ultrasound Med, 2021, 40(3): 513-520.

[17] Wu HY, Wang C, An Q, et al. Comparing the accuracy of shear wave elastography and strain elastography in the diagnosis of breast tumors: a systematic review and meta-analysis[J]. Medicine, 2022, 101(44): e31526.

[18] Golatta M, Pfob A, Büsch C, et al. The potential of combined shear wave and strain elastography to reduce unnecessary biopsies in breast cancer diagnostics - An international, multicentre trial[J]. Eur J Cancer, 2022, 161: 1-9.

[19] Bi WP, Shi Y, Wang LL, et al. Clinical value of ultrasonography combined with shear wave elastography for theassessment of molecular subtypes of breast cancer[J]. Chinese Journal of General Practice, 2023,21(12):2009-2013. **[In Chinese]**

[20] Xin BY, Dong M, Fu CH, et al. Differentiate diagnostic value of strain elastography technology for breast BI-RADS 4A type nodules[J]. China Med Her,2023,20(34):180-184. **[In Chinese]**

[21] Misra S, Jeon S, Managuli R, et al. Bi-modal transfer learning for classifying breast cancers via combined B-mode and ultrasound strain imaging[J]. IEEE Trans Ultrason Ferroelectr Freq Control, 2022, 69(1): 222-232.

[22] Zhang Q, Song S, Xiao Y, et al. Dual-mode artificially-intelligent diagnosis of breast tumours in shear-wave elastography and B-mode ultrasound using deep polynomial networks[J]. Med Eng Phys, 2019, 64: 1-6.

[23] Choi JS, Han BK, Ko ES, et al. Effect of a deep learning framework-based computer-aided diagnosis system on the diagnostic performance of radiologists in differentiating between malignant and benign masses on breast ultrasonography[J]. Korean J Radiol, 2019, 20(5): 749-758.

[24] Wang YQ, Tang L, Chen PP, et al. The role of a deep learning-based computer-aided diagnosis system and elastography in reducing unnecessary breast lesion biopsies[J]. Clin Breast Cancer, 2023, 23(3): e112-e121.

Submission received: 2023-12-07 / **Revised:**2024-01-29

·论　著·

双模态超声深度学习预测模型诊断乳腺癌的应用

李晓洁[1]，　赵国家[2]，　任金河[2]

1. 锦州医科大学临沂市人民医院研究生培养基地，山东 临沂 276000；2. 临沂市人民医院超声医学科，山东 临沂 276000

摘要：目的　采用基于乳腺超声灰阶图像和弹性图像的深度学习（DL）技术构建一个预测模型，并探讨该模型在乳腺病灶良恶性鉴别中的诊断效能。**方法**　回顾性收集 2020 年 5 月至 2021 年 4 月于临沂市人民医院乳腺外科接受手术治疗患者的乳腺病灶共 1 000 个，包括超声图像及相关临床病理资料，选择每个病灶最大切面的超声灰阶图像及弹性图像，按照 7∶2∶1 的比例随机将病灶分为训练集、验证集和测试集；应用训练集和验证集的病灶图像基于神经网络构建预测模型，应用测试集病灶图像检测模型的诊断效能；邀请四位超声医生分别阅读测试集病灶的超声图像，比较模型与不同年资医生之间的诊断效能。**结果**　DL 预测模型对乳腺病灶诊断的受试者工作特征曲线（ROC）曲线下面积（AUC）值（0.907）高于所有医生，差异有统计学意义（$P<0.05$）；高年资医生单独阅片诊断的平均 AUC 值（0.835）高于低年资医生（0.719），差异有统计学意义（$P<0.05$）。模型辅助低年资医生诊断测试集乳腺病灶平均 AUC 值为 0.806，模型辅助高年资医生诊断测试集乳腺病灶平均 AUC 值为 0.864，经过模型辅助阅片后，不同年资医生的诊断效能均有提升，对低年资医生 AUC 值提升幅度更明显，差异有统计学意义（$P<0.05$）。DL 模型辅助低年资医生阅片后其 AUC 值与高年资医生单独阅片 AUC 值比较差异无统计学意义（$P>0.05$）。**结论**　基于双模态超声 DL 预测模型可以显著提高医生对乳腺病灶良恶性鉴别的诊断效能。

关键词：深度学习；神经网络；乳腺癌；超声；灰阶图像；弹性成像；预测模型；人工智能

中图分类号：R737.9　TP391.4　**文献标识码：**A　**文章编号：**1674-8182(2024)03-0365-06

Application of dual-modality ultrasound deep learning predictive model in diagnosing breast cancer

LI Xiaojie*, ZHAO Guojia, REN Jinhe

** Jinzhou Medical University Linyi People's Hospital Postgraduate Traning Base, Linyi, Shandong 276000, China*

Corresponding author: REN Jinhe, E-mail: renjh8677@163.com

Abstract: Objective　To develop a predictive model using deep learning (DL) techniques based on breast ultrasound grayscale images and elastography, and to explore the diagnostic efficacy of this model in differentiating benign from malignant breast lesions. **Methods**　Data of 1 000 breast lesions from patients who underwent surgical treatment at Linyi People's Hospital Breast Surgery Department from May 2020 to April 2021 were collected retrospectively. including ultrasound images and related clinical pathological information. The ultrasound grayscale image and elastography of the largest section of each lesion were selected and randomly divided into training, validation, and test sets at a ratio of 7∶2∶1. A predictive model was constructed based on neural networks using the training and validation sets, and the diagnostic efficacy of the model was tested with the test set images. Four sonographers were invited to read the test set ultrasound images independently, and their diagnostic efficacies were compared with the model's performance. **Results** The area under the curve (AUC) value (0.907) of the receiver operating characteristic curve (ROC) of DL model for breast lesion diagnosis was higher than all participating sonographers, with a statistically significant difference ($P<0.05$). The average AUC value for the diagnosis by senior sonographers (0.835) was higher than that for junior sonographers (0.719), with a statistically significant difference ($P<0.05$). When the model assisted junior sonographers and senior sonographers in diagnosing the test set breast lesions, the average AUC value was 0.806 and 0.864, respectively.

DOI: 10.13429/j.cnki.cjcr.2024.03.008

通信作者：任金河，E-mail: renjh8677@163.com

出版日期：2024-03-20

QR code for English version

After assistance from the model, the diagnostic efficacy of sonographers of different experience levels improved, with a more significant increase for junior sonographers ($P<0.05$). Notably, there was no statistically significant difference in the AUC values between the junior sonographers assisted by the DL model and the senior sonographers reading alone ($P>0.05$). **Conclusion**　A predictive model based on dual-modality ultrasound DL can significantly improve the diagnostic efficacy of sonographers in differentiating benign from malignant breast lesions.

Keywords: Deep learning; Neural network; Breast cancer; Ultrasound; Elastic imaging; Grayscale image; Prediction model; Artificial intelligence

乳腺癌是全球女性发病率最高的癌症，致死率较高，且发病人群趋向年轻化，早期精准诊断至关重要[1-2]。乳腺超声检查可以显示乳腺病灶的形态、边缘、生长方式、内部回声等各项基本特征，具有较高的诊断价值[3-4]；超声应变弹性成像可以反映乳腺病灶内部及周边组织的硬度信息，有利于提高乳腺癌诊断的特异度和准确度[5-7]。然而，超声检查存在一定的主观性，尤其对乳腺病灶各种超声基本特征的判定及硬度信息的评估在不同医生之间存在一定差异，比较依赖超声医生的操作技术及经验积累[8]。近年来，基于深度学习（deep learning, DL）的计算机辅助诊断（computer-aided diagnosis, CAD）技术迅速发展，在乳腺[9]、甲状腺[10]、肺[11]、脑[12]等医学影像处理分析领域中发挥重要作用。本研究拟基于乳腺病灶灰阶超声图像联合应变弹性图像采用 DL 技术构建预测模型，并评估其能否辅助医生提高诊断准确率。

1　资料与方法

1.1　一般资料　本研究回顾性收集 2020 年 5 月至 2021 年 4 月于临沂市人民医院乳腺外科就诊并接受手术治疗的 888 例乳腺疾病患者，年龄 13~81（44.6±11.8）岁；共纳入 1 000 个有确切病理诊断的病灶，其中良性 600 个，恶性 400 个。纳入标准：（1）超声图像能清晰且完整显示乳腺病灶。（2）临床及病理资料完整。本研究仅回顾性分析患者既有的临床影像与病理资料，不干预临床诊治，不涉及患者隐私，符合伦理学原则，获伦理审核豁免。

1.2　超声图像　采用 GE LogiqE9 超声诊断仪，频率为 6~15 MHz 的高频线阵探头 ML6-15，具备应变弹性成像功能。选取每个乳腺病灶最大直径切面的超声弹性图像，共 1 000 幅图像按 7∶2∶1 随机分为训练集（$n=700$）、验证集（$n=200$）及测试集（$n=100$）三组，每组病例良、恶性比均为 3∶2。

1.3　图像预处理　以弹性成像的取样框大小为标准，切割提取灰阶超声图像及弹性图像中包含病灶及其周围部分正常组织结构的图像，去除初始图像中有关医院和患者的相关信息、仪器成像参数、体表标记等内容，以备输入构建模型。见图 1。

1.4　构建预测模型　采用 ResNet-101 神经网络分别提取超声灰阶图像和弹性图像中的各种特征参数，将特征融合层添加到网络结构中以融合灰阶图像和弹性图像的特征图，最后通过分类输出层进行病灶良、恶性二分类预测。见图 2。训练集 700 个病灶的灰阶图像和弹性图像同时输入模型进行参数的训练，每幅图像均带有良、恶性的真实标签，验证集 200 个病灶的图像用于优化调整模型参数，运用五折交叉验证的方法，获取具有最佳诊断效能预测模型，命名为 DL 模型。模型训练应用 Pytorch1.2.0 实现，基于 8GB NVIDIA GeForce RTX 2080 GPU 平台。

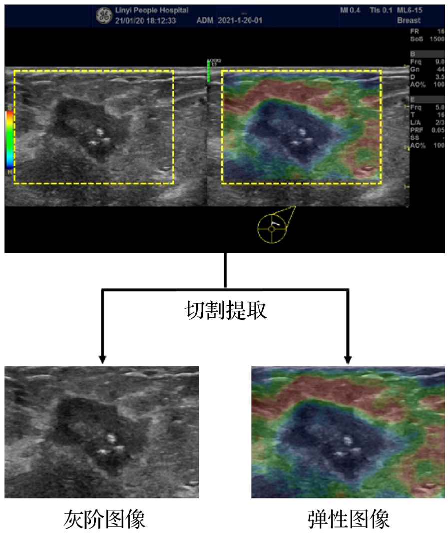

图 1　图像预处理

Fig. 1　Image preprocessing

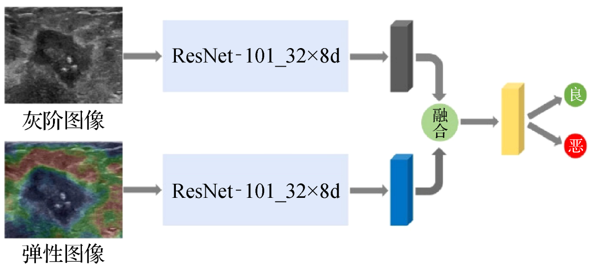

图 2　DL 模型特征提取融合

Fig. 2　Extraction and fusion of DL model feature

1.5　模型测试　测试集 100 个乳腺病灶的灰阶图像和弹性图像分别随机输入到 DL 模型中进行阅片诊断,评估模型的诊断效能。模型阅片诊断结果输出为每个病灶对应的恶性预测概率值(范围在 0~1 之间),以 0.5 为界值,大于等于 0.5 定义为可能恶性,标记为 1;小于 0.5 定义可能良性,标记为 0。

1.6　医生阅片　本研究邀请 4 位不同年资的超声医生采用双盲法进行阅片诊断。医生 1、2 分别具有 15 年、11 年乳腺超声诊断工作经验,将其归为高年资医生组;医生 3、4 分别具有 3 年、2 年乳腺超声诊断工作经验,将其归为低年资医生组。

阅片病例为测试集中 100 个乳腺病灶的灰阶超声图像和弹性图像,4 位医生分别在以下两种场景对每个病灶的超声图像进行阅片诊断:(1) 在没有 DL 模型辅助的场景单独阅片;(2) 在 DL 模型辅助的场景阅片。两次阅片间隔 4 周记忆洗脱期。DL 模型辅助阅片时医生参考模型对该病灶的恶性预测概率值及对应的预测诊断结果,可以选择接受或者拒绝模型提供的诊断结果。

1.7　统计学方法　应用 SPSS 26.0 和 MedCalc 14.0 统计学软件进行数据分析。计数资料以例(%)表示。以测试集乳腺病灶的病理诊断结果为金标准,分别计算 DL 模型和 4 位超声医生阅片诊断结果的敏感度、特异度、准确性、阳性预测值和阴性预测值。绘制受试者工作特征(receiver operating characteristic, ROC)曲线并计算曲线下面积(area under the curve, AUC),模型和不同医生之间的诊断效能差异比较使用 DeLong's 非参数检验。$P<0.05$ 为差异有统计学意义。

2　结　果

2.1　乳腺疾病患者和病灶的一般特征　训练集和测试集乳腺病灶的特征分布相似。良、恶性病灶的病理类型分布如表 1 所示。

2.2　DL 模型及不同年资医生单独或联合诊断效能比较　基于病灶的灰阶图像和超声弹性图像所构建的 DL 模型及不同年资医生对测试集 100 个病灶诊断结果的准确性、敏感度、特异度、阳性预测值和阴性预测值见表 2。ROC 曲线结果显示:(1) DL 模型对乳腺病灶诊断的 AUC 值高于所有医生,差异有统计学意义($P<0.05$);(2) 高年资医生单独阅片诊断的 AUC 值均高于低年资医生,差异有统计学意义($P<0.05$)。见图 3。

表 1　乳腺疾病患者病灶的一般特征　[例(%)]

Tab. 1　General characteristics of breast disease patients and lesions　[case(%)]

项目	训练集+验证集		测试集	
	良性	恶性	良性	恶性
病灶数	540	360	60	40
图像数[a]	1 080	720	120	80
病灶最大直径				
<10 mm	90(16.7)	22(6.1)	3(5.0)	3(7.5)
10~40 mm	443(82.0)	305(84.7)	55(91.7)	30(75.0)
>40 mm	7(1.3)	33(9.2)	2(3.3)	7(17.5)
BI-RADS				
3	386(71.5)	5(1.4)	41(68.3)	0
4a	118(21.9)	34(9.4)	14(23.3)	5(12.5)
4b	32(5.9)	81(22.5)	4(6.7)	9(22.5)
4c	4(0.7)	177(49.2)	1(1.7)	21(52.5)
5	0	63(17.5)	0	5(12.5)
病理诊断				
纤维腺瘤	405(75.0)		36(60.0)	
腺病	79(14.6)		9(15.0)	
导管内乳头状瘤	27(5.0)		3(5.0)	
乳腺炎	14(2.6)		5(8.3)	
硬化性腺病	5(0.9)		5(8.3)	
脂肪坏死	5(0.9)		1(1.7)	
叶状肿瘤	2(0.4)		1(1.7)	
浸润性导管癌		291(80.3)		34(85.0)
导管原位癌		53(14.7)		3(7.5)
黏液癌		6(1.7)		1(2.5)
混合性浸润癌		4(1.1)		1(2.5)
浸润性小叶癌		2(0.6)		1(2.5)
其他	3 (0.6)	4 (1.1)	0	0

注:[a] 表示每个病灶有灰阶和弹性 2 个图像。

表 2　DL 模型及不同年资医生单独或联合诊断效能比较　(%)

Tab. 2　Comparison of diagnostic performance of DL model and doctors with different years of experience, either alone or in conbination　(%)

项目	敏感度	特异度	准确性	阳性预测值	阴性预测值	AUC
DL 模型	82.5	83.3	83.0	87.7	76.7	0.907
医生 1	87.5	81.6	84.0	76.1	90.7	0.846
医生 2	85.0	80.0	82.5	73.9	88.9	0.825
医生 3	73.3	70.0	72.0	63.6	78.5	0.721
医生 4	57.5	81.6	72.0	67.6	74.2	0.717
DL+医生 1	90.0	85.0	87.0	80.0	92.7	0.875
DL+医生 2	87.5	83.3	85.0	77.7	90.9	0.854
DL+医生 3	80.0	81.6	81.0	74.4	85.9	0.804
DL+医生 4	82.5	78.3	80.0	71.7	87.0	0.808

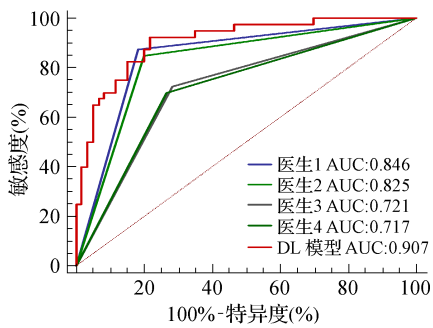

图 3　DL 模型和不同年资医生单独阅片诊断效能的 ROC 曲线

Fig. 3　ROC curves of diagnostic performance of DL model and doctors with different years of experience

2.3　DL 模型辅助医生阅片与医生单独阅片诊断效能比较　绘制模型辅助医生阅片及医生单独阅片诊断结果的 ROC 曲线，分别计算并比较每条曲线下面积 AUC 值。结果显示：(1) 经过模型辅助阅片后，不同年资医生的诊断效能均有提升，对低年资医生 AUC 值提升幅度更明显，差异有统计学意义(P<0.05)；对高年资医生 AUC 值提升效果有限，差异无统计学意义(P>0.05)；(2) DL 模型辅助低年资医生阅片后其诊断效能达到高年资医生单独阅片诊断的水平，两者 AUC 值比较差异无统计学意义(P>0.05)。见图 4。

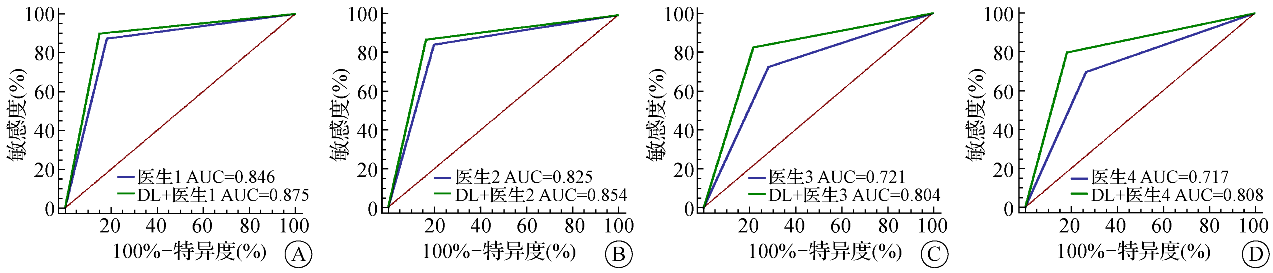

图 4　DL 模型辅助医生阅片和医生单独阅片诊断效能的 ROC 曲线
Fig. 4　ROC curve of the diagnostic performance of DL model in assisting doctors in reading films and doctors reading films individually

3　讨　论

乳腺超声广泛应用于临床，超声弹性成像可通过反映病灶及周围组织的硬度信息来提高乳腺癌的诊断准确性[4,13]。本研究所构建的 DL 模型对乳腺病灶的良恶性分类方面取得了令人满意的效果。

卷积神经网络(convolutional neural networks, CNN)的基本原理大致为训练一个核来识别特定的图像特征(卷积层)，然后该模型计算内核和输入图像之间的特征重叠程度(称为感受野)，随之是较高级别特征的汇聚层和完全连接的层以将数据扁平化为特征向量，模型的输出层通过密集网络和回归函数计算输出类的概率[14]。CNN 可从更多维度、更微观的像素级别对图像特征进行剖析，从而得到更准确的诊断，近年来，许多学者构建了针对乳腺病灶诊断的单模态 DL 模型，并与预期结果达到高度一致，有研究通过 CAD 基于常规二维超声图像对 266 个乳腺病灶进行诊断，结果显示 AUC 值高达 0.81，与有经验的超声医生的 AUC 值 0.82 相近，但高于经验较少 AUC 值为 0.76 的初级超声医生[15]。Li[16] 等构建了一个基于大数据集乳腺病灶的 DL 模型，并通过测试集病灶超声图像来评估模型的诊断效能，结果发现模型的诊断能力达到超声专家的水平，明显优于经验水平较低的医生(AUC 值为0.66~0.71，P<0.05)。但单纯基于病灶二维灰阶图像所构建的模型仅能提供病灶的基本二维有限信息，在此基础上，本研究在初始构建 DL 模型时还加入了病灶的弹性图像信息以争取模型得到更高的诊断效能。

Wu 等[17] 的一项荟萃分析中发现应用应变式弹性成像对乳腺病灶进行诊断 AUC 值高达 0.899。Golatta[18] 等通过对 1 288 名患有 BI-RADS 3 类到 4c 类乳腺病灶的女性进行超声检查，结果发现在常规超声的基础上加用弹性成像对 BI-RADS 4a 类患者进行重新分类，结果显示，可将乳腺诊断中不必要的活检次数减少约 35.35%，同时将恶性肿瘤的漏检率保持在 1.96%。以上均表明应用乳腺弹性成像技术可以丰富超声医生的诊断依据，从而得到更高效、准确的诊断。而临床中无论是采取弹性成像 5 分法或是应变比值的方法，诊断乳腺实性病灶过程中均存在人为主观性和重复差异性[19-20]，为了提高诊断的准确性、时效性以及减少观察者间的差异性，乳腺超声的 CAD 系统逐渐引入临床。在本研究中基于乳腺病灶二维灰阶图像及应变式超声弹性图像所构建的 DL 模型对乳腺病灶的分类取得了较为满意的结果，其诊断效能优于参与实验的不同年资医生(DL 模型和不同年资医生的 AUC 值分别为 0.907 和 0.717 ~ 0.846)。Misra[21]、Zhang 等[22] 的研究结果均表明基于乳腺常规二维灰阶超声图像和超声弹性图像所构建的双模态 DL 模型在乳腺病灶良恶性分类方面具有较高的诊断价值，本研究结果与其一致。由此笔者认为，基于加入弹性图像的 DL 模型比仅使用常规二维灰阶图像所构建的单模态模型更具乳腺病灶良恶性分类的能力。

本研究中应用 DL 模型辅助各位医生进行乳腺病灶诊断，即当医生与 DL 模型诊断结果不一致时，再次对病灶进行细致检查后，选择接受模型结果或是坚持之前的诊断，结果发现应用 DL 模型后各医生诊断 AUC 值均有所提升(辅助前及辅助后医生诊断平均 AUC 值分别为0.777和 0.835)。Choi[23] 等邀请四

名医生对 253 个乳腺病灶进行 BI-RADS 分类,当模型结果添加到常规超声时,其 AUC 值(0.91~0.95)显著高于仅使用常规超声图像的 AUC 值(0.88~0.92)。Wang[24]等在常规超声检查的基础上加用 CAD 和应变式弹性成像后,医生的 AUC 值从 0.72 显著提高到 0.91。综上,利用 DL 模型辅助医生进行超声诊断,可以一定程度上影响诊断者的决策,减少漏诊误诊,提高乳腺癌的检出率。

尽管本研究构建的 DL 模型在鉴别乳腺病灶良恶性方面表现出很高的诊断价值,但仍存在一定局限性:(1) 本研究建模时只纳入乳癌病灶的灰阶及弹性图像信息,未结合病灶的血流、造影情况及动态图像等信息。(2) 乳腺病灶为三维立体结构,本研究只纳入了病灶二维灰阶及超声弹性图像的纵横切面两幅静态图像,未涉及病灶冠状切面图像信息,在收集图像时可能会因超声医生的人为主观性导致结果存在偏差。(3) 本研究只纳入了乳腺占位性病变图像,对乳腺非占位性病变未收集纳入,可能会导致模型诊断效能偏高。

乳腺常规超声联合 CAD 将 DL 技术应用于乳腺病灶的检查,可以弥补由于医生经验、技术不足所导致的漏诊及误诊,提高医生的诊断效能。可将具有强大的学习能力和高效的分类性能等优势的 DL 方法应用到医院常规乳腺超声病灶检测和病变分类中。

利益冲突　无

参考文献

[1] Sung H, Ferlay J, Siegel RL, et al. Global cancer statistics 2020: GLOBOCAN estimates of incidence and mortality worldwide for 36 cancers in 185 countries[J]. CA Cancer J Clin, 2021, 71(3): 209-249.

[2] 赫捷,陈万青,李霓,等.中国女性乳腺癌筛查与早诊早治指南(2021,北京)[J].中华肿瘤杂志,2021,43(4):357-382.
He J, Chen WQ, Li N, et al. China guideline for the screening and early detection of female breast cancer(2021, Beijing)[J]. Chin J Oncol, 2021, 43(4): 357-382.

[3] Berg WA, Bandos AI, Mendelson EB, et al. Ultrasound as the primary screening test for breast cancer: analysis from ACRIN 6666 [J]. J Natl Cancer Inst, 2015, 108(4): djv367.

[4] Zanello PA, Robim AFC, Oliveira TM, et al. Breast ultrasound diagnostic performance and outcomes for mass lesions using Breast Imaging Reporting and Data System category 0 mammogram[J]. Clinics, 2011, 66(3): 443-448.

[5] Pfob A, Sidey-Gibbons C, Barr RG, et al. Intelligent multi-modal shear wave elastography to reduce unnecessary biopsies in breast cancer diagnosis (INSPiRED 002): a retrospective, international, multicentre analysis[J]. Eur J Cancer, 2022, 177: 1-14.

[6] 赵巧英,赵冰,吴刚,等.超声剪切波弹性成像定量参数对乳腺癌系统性治疗后局部区域复发的预测价值[J].中华实用诊断与治疗杂志,2023,37(4):377-382.
Zhao QY, Zhao B, Wu G, et al. Value of quantitative parameters of ultrasound shear wave elastography to the prediction of loco-regional recurrence of breast cancer after systemic therapy[J]. J Chin Pract Diagn Ther, 2023, 37(4): 377-382.

[7] 董梦,张秉宜,邢博缘.超声弹性成像技术在乳腺疾病中的应用进展[J].中国医药导报,2022,19(22):42-45,61.
Dong M, Zhang BY, Xing BY. Application progress of ultrasound elastography in breast diseases[J]. China Med Her, 2022, 19(22): 42-45, 61.

[8] Secco GM, Gutierrez PA, Secco VL, et al. Is breast ultrasound a good alternative to magnetic resonance imaging for evaluating implant integrity? [J]. Radiologia, 2022, 64 Suppl 1: 20-27.

[9] Yoon J, Lee HS, Kim MJ, et al. AI-CAD for differentiating lesions presenting as calcifications only on mammography: outcome analysis incorporating the ACR BI-RADS descriptors for calcifications[J]. Eur Radiol, 2022, 32(10): 6565-6574.

[10] Xie F, Luo YK, Lan Y, et al. Differential diagnosis and feature visualization for thyroid nodules using computer-aided ultrasonic diagnosis system: initial clinical assessment[J]. BMC Med Imaging, 2022, 22(1): 153.

[11] Shafi I, Din S, Khan A, et al. An effective method for lung cancer diagnosis from CT scan using deep learning-based support vector network[J]. Cancers, 2022, 14(21): 5457.

[12] Ishihara M, Shiiba M, Maruno H, et al. Detection of intracranial aneurysms using deep learning-based CAD system: usefulness of the scores of CNN's final layer for distinguishing between aneurysm and infundibular dilatation[J]. Jpn J Radiol, 2023, 41(2): 131-141.

[13] 王虎霞,龙胜潭,宋张骏,等.超声引导定位技术对乳腺肿瘤的诊断价值[J].中国临床研究, 2022, 35(9):1227-1232.
Wang HX, Long ST, Song ZJ, et al. Ultrasound-guided localization technique in the diagnosis of breast tumors[J]. Chin J Clin Res, 2022, 35(9): 1227-1232.

[14] Mao YJ, Lim HJ, Ni M, et al. Breast tumour classification using ultrasound elastography with machine learning: a systematic scoping review[J]. Cancers, 2022, 14(2): 367.

[15] Litjens G, Kooi T, Bejnordi BE, et al. A survey on deep learning in medical image analysis[J]. Med Image Anal, 2017, 42: 60-88.

[16] Li JM, Bu YY, Lu SQ, et al. Development of a deep learning-based model for diagnosing breast nodules with ultrasound [J]. J Ultrasound Med, 2021, 40(3): 513-520.

[17] Wu HY, Wang C, An Q, et al. Comparing the accuracy of shear wave elastography and strain elastography in the diagnosis of breast tumors: a systematic review and meta-analysis[J]. Medicine, 2022, 101(44): e31526.

[18] Golatta M, Pfob A, Büsch C, et al. The potential of combined shear wave and strain elastography to reduce unnecessary biopsies in breast cancer diagnostics-An international, multicentre trial[J]. Eur J Cancer, 2022, 161: 1-9.

(下转第 374 页)

270-276.

[5] Bolf EL, Gillis NE, Barnum MS, et al. The thyroid hormone receptor-RUNX2 axis: a novel tumor suppressive pathway in breast cancer [J]. Horm Cancer, 2020, 11(1): 34-41.

[6] Klubo-Gwiezdzinska J. Thyroid hormones enhance the growth of estrogen receptor-positive breast cancers[J]. Clin Thyroidol, 2022, 34(7): 286-289.

[7] Shin S, Sawada N, Saito E, et al. Menstrual and reproductive factors in the risk of thyroid cancer in Japanese women: the Japan Public Health Center-Based Prospective Study[J]. Eur J Cancer Prev, 2018, 27(4): 361-369.

[8] Sebastian W, Forchette L, Donoughe K, et al. Genetics, treatment, and new technologies of hormone receptor-positive breast cancer[J]. Cancers, 2023, 15(4): 1303.

[9] Lalitkumar PGL, Lundström E, Byström B, et al. Effects of estradiol/micronized progesterone *vs*. conjugated equine estrogens/medroxyprogesterone acetate on breast cancer gene expression in healthy postmenopausal women[J]. Int J Mol Sci, 2023, 24(4): 4123.

[10] Camejo N, Castillo C, Tambasco C, et al. Assessing adherence to adjuvant hormone therapy in breast cancer patients in routine clinical practice[J]. World J Oncol, 2023, 14(4): 300-308.

[11] Bozovic-Spasojevic I, Zardavas D, Brohée S, et al. The prognostic role of androgen receptor in patients with early-stage breast cancer: a meta-analysis of clinical and gene expression data[J]. Clin Cancer Res, 2017, 23(11): 2702-2712.

[12] Hu XQ, Chen WL, Ma HG, et al. Androgen receptor expression identifies patient with favorable outcome in operable triple negative breast cancer[J]. Oncotarget, 2017, 8(34): 56364-56374.

[13] 韩云云,武新宇,李博,等.包含分化型甲状腺癌的双原发恶性肿瘤患者临床特征及生存分析[J].中华实用诊断与治疗杂志,2023,37(1):101-104.
Han YY, Wu XY, Li B, et al. Clinical characteristics and survival analysis of dual primary malignancies containing differentiated thyroid cancer[J]. J Chin Pract Diagn Ther, 2023, 37(1): 101-104.

[14] 杨海波,高晋南,宋宛芝.单纯乳腺癌与乳腺癌合并甲状腺癌患者临床病理特征分析[J].中华肿瘤杂志,2019,41(8):624-627.
Yang HB, Gao JN, Song WZ. Analysis of clinicopathological features of patients with simple breast cancer and breast cancer with thyroid cancer[J]. Chin J Oncol, 2019, 41(8): 624-627.

收稿日期:2023-10-19　**编辑**:王国品

(上接第369页)

[19] 毕伟培,石彦,王玲玲,等.超声造影联合剪切波弹性成像评估乳腺癌分子亚型的临床价值[J].中华全科医学,2023,21(12):2009-2013.
Bi WP, Shi Y, Wang LL, et al. Clinical value of ultrasonography combined with shear wave elastography for theassessment of molecular subtypes of breast cancer[J]. Chinese Journal of General Practice, 2023,21(12): 2009-2013.

[20] 邢博缘,董梦,付承辉等.应变式弹性成像技术对乳腺BI-RADS 4A类结节的鉴别诊断价值[J].中国医药导报,2023,20(34):180-184.
Xin BY, Dong M, Fu CH, et al. Differentiate diagnostic value of strain elastography technology for breast BI-RADS 4A type nodules [J]. China Med Her, 2023, 20(34): 180-184.

[21] Misra S, Jeon S, Managuli R, et al. Bi-modal transfer learning for classifying breast cancers via combined B-mode and ultrasound strain imaging[J]. IEEE Trans Ultrason Ferroelectr Freq Control, 2022, 69(1): 222-232.

[22] Zhang Q, Song S, Xiao Y, et al. Dual-mode artificially-intelligent diagnosis of breast tumours in shear-wave elastography and B-mode ultrasound using deep polynomial networks[J]. Med Eng Phys, 2019, 64: 1-6.

[23] Choi JS, Han BK, Ko ES, et al. Effect of a deep learning framework-based computer-aided diagnosis system on the diagnostic performance of radiologists in differentiating between malignant and benign masses on breast ultrasonography[J]. Korean J Radiol, 2019, 20(5): 749-758.

[24] Wang YQ, Tang L, Chen PP, et al. The role of a deep learning-based computer-aided diagnosis system and elastography in reducing unnecessary breast lesion biopsies[J]. Clin Breast Cancer, 2023, 23(3): e112-e121.

收稿日期:2023-12-07　**修回日期**:2024-01-29　**编辑**:王娜娜